Insights into self-assembling nanoporous peptide and *in situ* reducing agent†

Poulami Jana, Sibaprasad Maity and Debasish Haldar*

Received 28th April 2010, Accepted 14th September 2010
DOI: 10.1039/c0ce00143k

A tripeptide containing an Aib (α-amino isobutyric acid) residue self-assembles to form porous nanomaterials in solid state. In spite of having a hollow nanotubular structure, the self-assembly nature of the peptide is different, which leads to the formation of pores with different internal diameters. The single-crystal X-ray diffraction study reveals that the peptide forms continuous hydrogen-bonded polydisperse nanopores (3, 5 and 8 membered) starting from the β-turn conformation as an associating subunit. The field emission scanning electron micrograph (FESEM) shows that the average pore sizes are in the range of 20 to 200 nm, although a few large pores are also visible. Moreover, the peptide **1** acts as an *in situ* reducing agent to synthesize hexagonal gold nanoparticles (GNP).

Introduction

Nanoporous materials having unique bulk, surface and structural properties are an emerging area of current research due to their potential importance in various fields, like catalysis, sensors, ion exchange, separation, purifications and bio-molecular isolation.[1] Depending on the size, microporous (pore size below 2 nm), mesoporous (2–50 nm) and macroporous (exceeding 50 nm) solids can be constructed efficiently from a single molecule or ionic template or the molecular recognition and association of organic templates.[2] The nanoporous materials have a wide propensity to interact with atoms, ions and molecules, which adsorb on their nanometre sized pore space and in the large interior surfaces.[3] Over the last few decades, enormous efforts have been devoted to the synthesis and characterization of nanoporous materials with a uniform pore size and pore structure due to their attractive textual and structural features, such as highly ordered structures, tuneability and ultra-high surface areas.[4] However, a hybrid material containing both interconnected macroporous and mesoporous structures have enhanced properties compared with single-sized pore materials due to the increased mass transport through the material and the maintenance of a specific surface area on the level of fine pore systems.[5] Many studies have been made of inorganic microporous materials, such as zeolites, which have well-defined network structures of silicon and aluminium atoms linked *via* oxygen atoms.[6] But, it has proved difficult to form organic polymer networks with perfectly controlled pore dimensions.[7] Most of the reports consist of metal–organic frameworks, in which rigid organic components are linked by noncovalent interactions, such as metal–ligand or hydrogen bonds.[8] Surfactants and amphiphilic copolymers can be used as templates to synthesize ordered mesoporous materials[9] and periodic three-dimensional arrays of macropores have been fabricated using latex spheres as templates.[10] Yaghi and co-workers have reported the development of highly porous, organic, three-dimensional crystalline covalent networks.[11] We are developing nanostructured materials by molecular recognition and self-association of peptides and oligoamides.[12]

There has been tremendous interest in recent times in assembling nanoparticles in close-packed aggregates because of their unusual optoelectronic and chemical properties,[13]which have potential applications in nanoelectronics,[14] bio-analytical processes[15] and catalysis.[16] Among these, gold nanoparticles (GNPs) are of much contemporary interest and have been extensively investigated.[17] Generally GNPs are prepared by the reduction of HAuCl4 with NaBH4 or citrate in presence of a stabilizer,[16,18] but the by- product of these reducing agents and the stabilizer may create complications when used in some bio-analytical applications. Therefore, the *in situ* reduction technique is important in order to avoid this problem.[19]

Herein we have analyzed by means of field emission scanning electron microscopy and single-crystal X-ray crystallography, the formation of a novel supramolecular nanoporous material from a terminally blocked tripeptide Boc-Tyr(1)-Aib(2)-Val(3)-OMe **1**, which self-associates, exploiting the hydrogen-bonding functionalities of the peptide bonds. Moreover, the peptide **1** acts as an *in situ* reducing agent in the synthesis of hexagonal gold nanoparticles.

Results and discussion

Synthesis and FTIR analysis

The tripeptide Boc-Tyr(1)-Aib(2)-Val(3)-OMe **1** has been synthesized by conventional solution phase methodology[20] (ESI, Fig. S1†) and purified, characterized and studied. The terminally protected tripeptide **1** contains a helicogenic α-amino isobutyric acid residue[21] at a central position. Solid-state FTIR spectroscopy was performed to study the secondary structure of the peptide **1**. The region 1800–1500 cm^{-1} is important for the stretching band of amide I, the bending peak of amide II and the hydrogen bonded urethane groups.[22] Another informative frequency range is 3500–3200 cm^{-1}, corresponding to the N–H stretching vibrations of the peptide.[22] The FTIR study shows that the peptides molecules are strongly intermolecularly

Department of Chemical Sciences, Indian Institute of Science Education and Research – Kolkata, Mohanpur, West Bengal 741252, India. E-mail: deba_h76@yahoo.com; deba_h76@iiserkol.ac.in; Fax: +91-34-73 279131; Tel: +91-34-73 279130

† Electronic supplementary information (ESI) available: Crystallographic file, ^{1}H-NMR, ^{13}C NMR, HRMS spectra. CCDC reference number 753226. For ESI and crystallographic data in CIF or other electronic format see DOI: 10.1039/c0ce00143k

hydrogen bonded in the solid state (ESI, Fig. S2†). An intense band at 3272 cm^{-1} and 3291 cm^{-1} were observed for the reported peptide, indicating the presence of strongly hydrogen-bonded NH groups. No band has been observed at around 3400 cm^{-1}, indicating that all NH groups are involved in intermolecular hydrogen bonding.[23] The characteristic IR absorption bands at about 1567, 1616, 1645, 1675, 1699 and 1727 cm^{-1} suggest that the peptides have no distinguished structure, such as the typical parallel or antiparallel β-sheet or helical structures.[24]

Crystallographic analysis

The colourless orthorhombic crystals of peptide **1**, suitable for single-crystal X-ray diffraction analysis, were obtained from a methanol–water solution by slow evaporation. The molecular conformation of peptide **1** in the crystal is represented in Fig. 1. From Fig. 1 it is evident that there is an intramolecular hydrogen bond between the BOC C═O and the Val NH, resulting in a ten membered hydrogen-bonded β-turn conformation in the solid state.[25] The backbone torsion angles of peptide **1** (Table 1) reveal that the turn is of Type II or β-turn. The Aib(2) residue occupies the $i + 2$ position of the β-turn. The individual β-turn sub-units of this peptide are themselves regularly inter-linked *via* multiple intermolecular hydrogen bonds N1-H111···O1, N3-H333···O7 and O2–H2···O6 and thereby form a three membered supramolecular nanopore along the crystallographic *b* axis direction (Fig. 2). The average internal diameter for the three membered pore is 7.7 Å. The β-turn-containing peptide **1** sub-unit has the potential to further self-assemble into a five membered supramolecular pore-like structure in the solid state. In this case, the molecules are bound by five intermolecular hydrogen bonds N1–H111···O1, N3–H333···O7 and three O2–H2···O6 bonds, along the crystallographic *c* axis direction (Fig. 3). Moreover, the packing diagram shows that there is also the possibility to form an 8 membered supramolecular porous structure (Fig. 4) through intermolecular hydrogen bonds along the crystallographic *c* axis. There are eight intermolecular hydrogen bonds (four N1–H111…O1, three N3–H333…O7 and one O2–H2…O6) that are responsible for connecting individual molecules in order to create and stabilize the moderate-size pore-like self-assemblage. The hydrogen bonding parameters of peptide **1** are listed in Table 2.

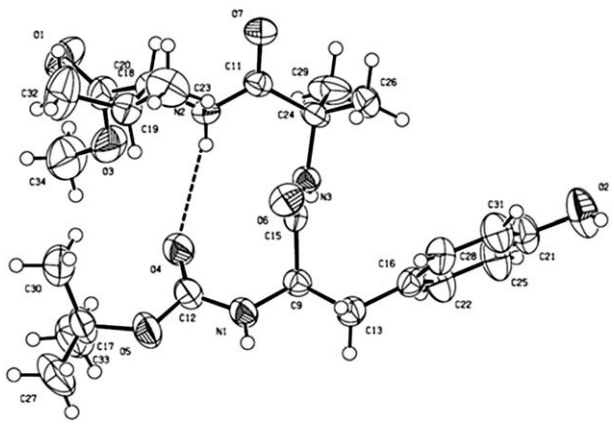

Fig. 1 The ORTEP diagram of tripeptide **1** showing the atomic numbering scheme. Ellipsoids are drawn at the 30% probability level. Intramolecular hydrogen bond is shown as a dotted line.

Table 1 Selected backbone torsion angles (°) for peptide **1**

C9-N1-C12-O5	179.44	ω_0	N2-C11-C24-N3	−16.10	ψ_2
C12-N1-C9-C15	53.07	ϕ_1	C9-N2-C11-C24	−171.25	ω_2
N1-C9-C15-N3	−128.03	ψ_1	C11-N2-C20-C18	131.15	ϕ_3
C24-N3-C15-C9	−171.25	ω_1	O1-C18-C20-N2	−145.92	ψ_3
C15-N3-C24-C11	−67.70	ϕ_2			

Morphology and characterization

To obtain insight about the morphology of the reported peptide, field-emission scanning electron microscopic (FE-SEM) measurements were carried out.[26] For FE-SEM experiments, dilute solutions (0.5 mM) of tripeptide **1** in methanol–water (1 : 1 v/v) were placed on a microscopic glass slide and then dried under vacuum for two days. Fig. 5 depicts the FE-SEM image of the peptide. From Fig. 5, the micrograph shows the porous nanostructure morphology in the self-assembled state and the pores are polydisperse in nature with different diameters. Average pores size are 20–200 nm. These values are much higher than the values obtained from single-crystal X-ray

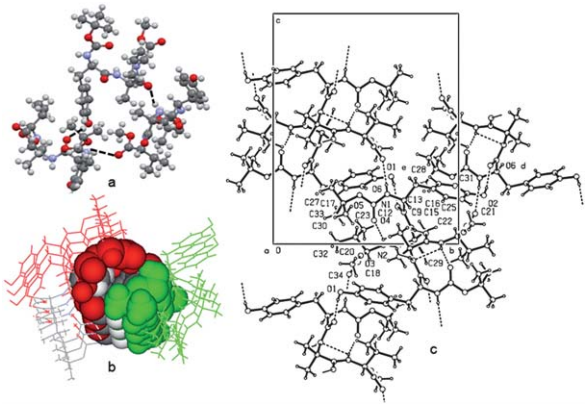

Fig. 2 The three membered nanopore (a) in ball and stick model, (b) space-filling representation showing higher-ordered supramolecular assembly along the crystallographic *b* direction, (c) packing of the tripeptide **1** in a higher order assembly. Hydrogen bonds are shown as dotted lines.

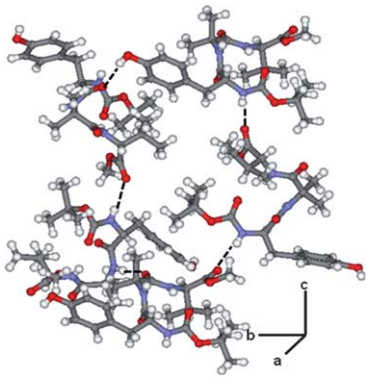

Fig. 3 The ball and stick presentation of five membered nanopore along crystallographic *c* axis direction. Hydrogen bonds are shown as dotted lines. Nitrogen atoms are blue, oxygen atoms are red and carbon atoms are gray.

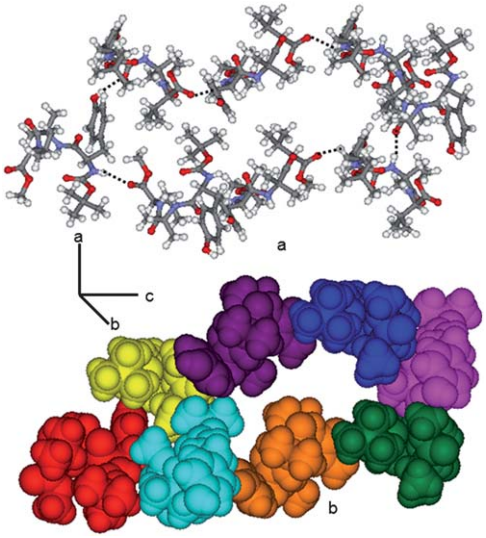

Fig. 4 The nanopore obtained by self-assembly of eight β-turn subunits along the *c* axis direction.

Table 2 Hydrogen bonding parameters of peptide **1**[a]

D–H···A	H···A/Å	D···A/Å	D–H···A/°
O2–H2···O6b	1.98	2.71	169.00
N1–H111···O1e	2.29	3.04	169.00
N2–H222···O4	2.46	3.20	162.00
N2–H222···N3	2.41	2.77	110.00
N3–H333···O7f	2.00	2.89	171.00

[a] Symmetry equivalent: $b = [4655.00] = 1 - x, 1/2 + y, 1/2 - z$, $e = [2554.00] = 1/2 - x, -y, -1/2 + z$, $f = [3456.00] = -1/2 + x, 1/2 - y, 1 - z$.

crystallography. This indicates that the self-assembled states are actually the supramolecular clusters of several molecules. Further BET analysis[27] of the crystallized peptide **1** (degassed at 150 °C) exhibits more information about the pore size dimensions of the nanoporous material (ESI, Fig. S3 and S4†).[28]

Synthesis and characterization of GNP

Previous reports have demonstrated that gold nanoparticles have been synthesized using tyrosine, alkylated tyrosine and tyrosine-based peptides.[29] Incorporating the redox active tyrosine residue into the nanopore forming tripeptides template, we want to fabricate the *in situ* synthesis of gold nanoparticles. The following method was used for the synthesis of the gold nanoparticles with peptide **1**. An aqueous yellow coloured solution (0.5 mL) of $HAuCl_4$ (20 mg in 2 mL) was added to the methanol–water (1 : 0.5 v/v) solution of the peptide **1** (1 mg mL^{-1}) and was stirred to produce a homogeneous solution. The yellow coloration of the mixture was not changed for several days. NaOH solution (2 M) was added dropwise into the yellow solution to adjust the pH at 9. Immediately the yellow colour changed to a colourless solution [Au(III) to Au(I)] and finally it turned into a violet solution within a few minutes indicating the formation of gold nanoparticles [Au(0)] *via* the oxidation of the tyrosine residues of peptide **1**. The presence of a surface Plasmon band at around 548 nm suggests the existence of gold nanoparticles (ESI, Fig. S5†).[29] Field-emission scanning electron microscopy was used to characterize the gold nanoparticles. A drop of the violet coloured gold nanoparticle solution (methanol–water 1 : 1) was placed on a microscopic glass slide and it was allowed to dry under reduced pressure at room temperature for two days. Fig. 6 shows the image of the gold nanoparticles with a hexagonal shape, with various particle sizes ranging from 50 nm to 80 nm in diameter.

Experimental

General methods and materials

All L-amino acids (L-tyrosine, L-valine and α-amino isobutyric acid) were purchased from Sigma chemicals. HOBt (1-hydroxybenzotriazole) and DCC (dicyclohexylcarbodiimide) were purchased from SRL.

Synthesis

The peptides were synthesized by conventional solution-phase methodology, by using a racemization free fragment condensation strategy (see the ESI† for detailed synthetic procedure). The Boc group was used for N-terminal protection and the C-terminus was protected as a methyl ester. Couplings were mediated by dicyclohexylcarbodiimide–1-hydroxybenzotriazole (DCC–HOBt). Deprotection of the methyl ester was performed using the saponification method. All of the intermediates were

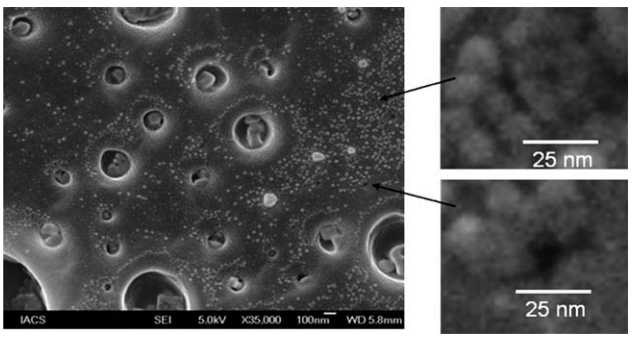

Fig. 5 FE-SEM image of tripeptide **1** showing nanoporous morphology in the solid state.

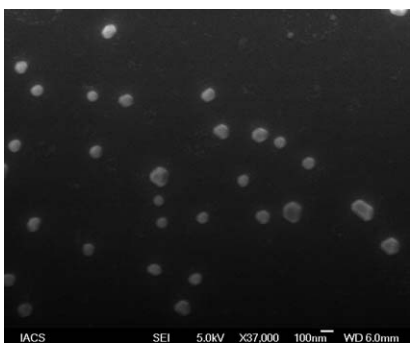

Fig. 6 FE-SEM image of hexagonal gold nanoparticles obtained by the *in situ* reducing properties of tripeptide **1**.

characterized by 500 MHz ^{1}H NMR and mass spectrometry. The final compound was fully characterized by 500 MHz ^{1}H NMR spectroscopy, ^{13}C NMR spectroscopy (125 MHz), mass spectrometry and IR spectroscopy. The peptide **1** was characterized by single-crystal X-ray crystallography.

(a) Boc-Tyr-OH. A solution of L-tyrosine (3.62 g, 20 mmol) in a mixture of dioxane (40 mL), water (20 mL) and 1M NaOH (20 mL) was stirred and cooled in an ice–water bath. Di-*tert*-butylpyrocarbonate (4.8 g, 22 mmol) was added and stirring was continued at room temperature for 6 h. Then the solution was concentrated under vacuum to about 20–30 mL, cooled in an ice–water bath, covered with a layer of ethyl acetate (about 50 mL) and acidified with a dilute solution of $KHSO_4$ to pH 2–3 (congo red). The aqueous phase was extracted with ethyl acetate and this operation was done repeatedly. The ethyl acetate extracts were pooled, washed with water and dried over anhydrous Na_2SO_4 and evaporated under vacuum. The pure material was obtained as a waxy solid. Yield 4.87 g (17 mmol, 85%). ^{1}H NMR (500MHz, $CDCl_3$, δ in ppm): 12.75 (br, 1 H, –COOH), 9.21 (s, 1 H, Tyr –OH), 7.02–7.00 (d, 2 H, J = 10 Hz, Tyr phenyl ring protons), 6.65–6.63 (d, 2 H, J = 10 Hz, Tyr phenyl ring protons), 4.04 (m, 1 H, Tyr C$^{\alpha}$ H), 3.91 (d, 1 H, J = 8 Hz, Tyr NH), 2.88 (m, 2 H, Tyr C$^{\beta}$ H), 1.42 (s, 9 H, BOC CH_3). ^{13}C NMR (125 MHz, $CDCl_3$, δ in ppm): 173.74, 155.78, 129.96, 127.98, 114.87, 55.50, 35.61, 28.13. Anal. calcd for $C_{14}H_{19}NO_5$ (281): C 59.78, H 6.81, N 4.98. Found: C 59.81, H 6.79, N 4.99.

(b) Boc-Tyr(1)-Aib(2)-OMe. 4.5 g (16 mmol) of Boc-Tyr-OH was dissolved in 25 mL DCM in an ice-water bath. H-Aib-OMe was isolated from 4.91 g (32 mmol) of the corresponding methyl ester hydrochloride by neutralization and subsequent extraction with ethyl acetate and the ethyl acetate extract was concentrated to 10 mL. It was then added to the reaction mixture, followed immediately by 3.3 g (16 mmol) dicyclohexylcarbodiimide (DCC) and 2.2 g (16 mmol) of HOBt. The reaction mixture was allowed to come to room temperature and stirred for 48 h. DCM was evaporated and the residue was dissolved in ethyl acetate (60 mL) and dicyclohexylurea (DCU) was filtered off. The organic layer was washed with 2M HCl (3 × 50 mL), brine (2 × 50 mL), 1M sodium carbonate (3 × 50 mL) and brine (2 × 50 mL) and dried over anhydrous sodium sulfate. It was evaporated in a vacuum to yield Boc-Tyr-Aib-OMe as a white solid. Yield 4.56 g (12 mmol, 75%). Mp.122–128 °C. ^{1}H NMR (500MHz, $CDCl_3$, δ in ppm): 9.21 (s, 1 H, Tyr –OH), 7.03–7.02 (d, 2 H, J = 5 Hz, Tyr phenyl ring protons), 6.75–6.74 (d, 2 H, J = 5 Hz, Tyr phenyl ring protons), 6.48 (s, 1 H, Aib(2) NH), 5.22 (d, 1 H, J = 5 Hz, Tyr NH), 4.22 (m, 1 H, Tyr C$^{\alpha}$ H), 3.70 (s, 3 H, –OCH_3), 2.95–2.90 (m, 2 H, Tyr C$^{\beta}$ H), 1.44 (s, 6 H, Aib C$^{\beta}$ H), 1.41 (s, 9 H, BOC CH_3). HRMS *m*/*z* 403.10 [M + Na]$^+$, *M*calcd 380.44. FTIR (KBr): 1519, 1595, 1682, 2852, 2932, 2982, 3063, 3329. ^{13}C NMR (125 MHz, $CDCl_3$, δ in ppm): 174.17, 170.74, 155.66, 130.58, 127.97, 115.56, 56.45, 53.45, 37.58, 29.70, 24.74. Anal. calcd for $C_{19}H_{28}N_2O_6$ (380): C 59.98, H 7.42, N 7.36. Found: C 60.01, H 7.38, N 7.38.

(c) Boc-Tyr(1)-Aib(2)-OH. To 4.4 g (12 mmol) of Boc-Tyr-Aib-OMe, 25 mL MeOH and 2M 15 mL NaOH were added and the progress of saponification was monitored by thin layer chromatography (TLC). The reaction mixture was stirred. After 10 h, methanol was removed under vacuum; the residue was dissolved in 50 mL of water and washed with diethyl ether (2 × 50 mL). Then the pH of the aqueous layer was adjusted to 2 using 1M HCl and it was extracted with ethyl acetate (3 × 50 mL). The extracts were pooled, dried over anhydrous sodium sulfate, and evaporated under vacuum to obtained compound as a waxy solid. Yield 3.8 g (10.38 mmol, 89.6%). ^{1}H NMR (500MHz, DMSO-d_6, δ in ppm): 12.75 (br, 1 H, –COOH), 9.14 (s, 1 H, Tyr –OH), 8.02 (s, 1 H, Aib(2) NH), 7.01–7.03 (d, 2 H, J = 10 Hz, Tyr phenyl ring protons), 6.66 (d, 1 H, J = 5 Hz, Tyr NH), 6.61–6.63 (d, 2 H, J = 10 Hz, Tyr phenyl ring protons), 4.01 (m, 1 H, Tyr C$^{\alpha}$ H), 2.78–2.81 (m, 2H, Tyr C$^{\beta}$ H), 1.34 (s, 3 H, Aib C$^{\beta}$ H), 1.32 (s, 3 H, Aib C$^{\beta}$ H), 1.30 (s, 9 H, BOC CH_3). HRMS *m*/*z* 405.66 [M + K]$^+$, *M*calcd 366.41. ^{13}C NMR (125 MHz, DMSO-d_6, δ in ppm): 175.43, 170.95, 155.64, 130.14, 128.02, 114.69, 177.91, 155.61, 28.10, 24.70. Anal. calcd for $C_{18}H_{26}N_2O_6$ (366): C 59.00, H 7.15, N 7.65. Found: C 58.98, H 7.18, N 7.63.

(d) Boc-Tyr(1)-Aib(2)-Val(3)-OMe. 3.7 g (10.1 mmol) Boc-Tyr-Aib–OH was dissolved in 10 mL of DMF in an ice–water bath. H-Val-OMe 3.34 g (20 mmol) was isolated from the corresponding methyl ester hydrochloride by neutralization and subsequent extraction with ethyl acetate and the ethyl acetate extract was concentrated to 7 mL. Then it was added to the reaction mixture, followed immediately by 2.08 g (10.11 mmol) of dicyclohexylcarbodiimide (DCC) and 1.37 g (10.11 mmol) of HOBt. The reaction mixture was allowed to come to room temperature and then stirred for 72 h. The residue was taken in 30 mL ethyl acetate and dicyclohexylurea (DCU) was filtered off. The organic layer was washed with 2 M HCL (3 × 50 mL), brine (2 × 50 mL), then 1 M sodium carbonate (3 × 30 mL) and brine (2 × 30 mL) and dried over anhydrous sodium sulfate and evaporated under vacuum to yield the tripeptide **1** as a white solid. Purification was done by silica gel column (100–200 mesh size) with an ethyl acetate and hexane mixture 1 : 2 as the eluent. Yield 4.4g (9.17 mmol, 90%). Mp. 140–143 °C. ^{1}H NMR (500MHz, DMSO-d_6, δ in ppm): 9.15 (s, 1 H, Tyr –OH), 7.93 (s, 1 H, Aib(2) NH), 7.28 (d, 1 H, J = 10 Hz, Val NH), 7.02–7.03 (d, 2 H, J = 5 Hz, Tyr phenyl ring protons), 6.89 (d, 1 H, J = 10 Hz, Tyr NH), 6.63–6.64 (d, 2 H, J = 5 Hz, Tyr phenyl ring protons), 4.14 (m, 1 H, Tyr C$^{\alpha}$ H), 4.05 (m, 1 H, Val C$^{\alpha}$ H), 3.62 (s, 3 H, -OCH_3), 2.92–3.03 (m, 2 H, Tyr C$^{\beta}$ H), 2.16–2.19 (m, 1 H, Val C$^{\beta}$ H), 1.31 (s, 9 H, BOC CH_3), 1.25 (s, 6 H, Aib C$^{\beta}$ H), 0.83 (d, 6 H, J = 10 Hz, Val C$^{\gamma}$ H). $[\alpha]_D^{27.8}$ −35.7 (*c* 2.10, $CHCl_3$). HRMS *m*/*z* 502.26 [M + Na]$^+$, *M*calcd 479.57. FTIR (KBr): 1518, 1532, 1567, 1616, 1645, 1675, 1699, 1727, 2969, 3086, 3273, 3346 cm^{-1}. ^{13}C NMR (125 MHz, $CDCl_3$, δ in ppm): 174.13, 172.38, 171.19, 155.40, 130.46, 127.83, 115.73, 57.54, 52.15, 37.37, 31.14, 28.27, 25.74, 24.56, 29.03, 17.80. Anal. calcd for $C_{24}H_{37}N_3O_7$ (479): C 60.11, H 7.78, N, 8.76. Found: C 60.07, H 7.73, N 8.80.

NMR experiments

All NMR studies were carried out on a Brüker AVANCE 500 MHz spectrometer at 298 K. The compounds concentrations were in the range 1–10 mmol in $CDCl_3$ and $(CD_3)_2SO$.

FTIR spectroscopy

All reported solid-state FTIR spectra were obtained with a Perkin Elmer Spectrum RX1 spectrophotometer with the KBr disk technique.

Mass spectrometry

Mass spectra were recorded on a Q-Tof Micro YA263 high-resolution (Waters Corporation) mass spectrometer by positive-mode electrospray ionization.

Polarimeter

Rudolph Research analytical instrument. Model Autopol IV Polarimeter was used.

Scanning electron microscopy

The morphologies of the reported materials were investigated by field emission scanning electron microscopy (FE-SEM). For the SEM study, the peptide solution (methanol–water 1 : 1 v/v) was drop cast on a clean and dry microscopic glass slide, dried and coated with platinum. Then the micrographs were taken in a SEM apparatus (JEOL Microscope JSM-6700F).

X-Ray crystallography

Single-crystal X-ray analysis of tripeptide **1** was recorded on a Bruker high resolution X-ray diffractometer instrument.

Crystallographic data

Crystal data for peptide 1: $C_{24}H_{37}N_3O_7$, $M_r = 479.57$, orthorhombic, crystal size 0.14 × 0.26 × 0.32 mm, spacegroup $P2_12_12_1$, $a = 10.840(10)$, $b = 14.535(13)$, $c = 18.079(16)$ Å, $U = 2849$ Å^3, $Z = 4$, $d_m = 1.118$ M g m^{-3} Intensity data were collected with Mo-Kα radiation at room temperature using Bruker APEX-2 CCD diffractometer. The crystal was positioned at 70 mm from the image plate. 100 frames were measured at 2° intervals with a counting time of 5 min to give 5000 independent reflections. Data were processed using the Bruker SAINT package and the structure solution and refinement procedures were performed using SHELX97.[30] The non-hydrogen atoms were refined with anisotropic thermal parameters. The hydrogen atoms were included in geometric positions and given thermal parameters equivalent to 1.2 times those of the atom to which they were attached. The final R values were R_1 0.0504 and wR_2 0.0919 for 3144 data with $I > 2\sigma(I)$. The largest peak and hole in the final difference Fourier were 0.20 and 0.54 eÅ^{-3}. The data have been deposited at the Cambridge Crystallographic Data Centre with reference number CCDC 753226.†

N_2 gas adsorption studies

Nitrogen adsorption–desorption isotherms were obtained using a Quantachrome Autosorb Automated Gas Sorption system at 77 K. The peptide **1** crystals were degassed at 150 °C for 4 h.

Conclusions

In conclusion, we have demonstrated the self-assembly of a tripeptide containing α-amino isobutyric acid to form porous nanomaterials in the solid state. The solid state FTIR study shows that the tripeptide **1** has a highly hydrogen bonded network but a lack of distinguished classical structure. These differences in the self-assembly nature of the peptides leads to the formation of pores with different internal diameters. The field-emission scanning electron microscopy reveals a porous nanostructure with average pore sizes in the range of 20 to 200 nm in the solid state. The single-crystal X-ray diffraction study shows that the peptide forms continuous hydrogen-bonded polydisperse nano pores (3, 5 and 8 membered) starting from the β-turn conformation as an associating sub-unit. Moreover, the peptide **1** acts as an *in situ* reducing agent and synthesizes hexagonal gold nanoparticles (GNP). The results presented here have formed a novel understanding of structure formation and will provide useful guidelines for the design of nanomaterials with predefined functionality.

Acknowledgements

We acknowledge the DST, New Delhi, India, for financial assistance Project No. (SR/FT/CS-041/2009). P. Jana and S. Maity wish to acknowledge the C.S.I.R, New Delhi, India for research fellowships. We are thankful to Dr Raju Mandal, Department of Inorganic Chemistry, I. A. C. S., Jadavpur, Kolkata 700032, India for his assistance in single-crystal X-ray crystallography data refinement. We gratefully acknowledge the I. A. C. S., Jadavpur, Kolkata 700032, India, for using the Mass Spectrometry, X-ray crystallography and FE-SEM facilities.

Notes and references

1 (*a*) A. Stein, *Adv. Mater.*, 2003, **15**, 763–775; (*b*) M. E. Davis, *Nature*, 2002, **417**, 813–821; (*c*) D. Zhao, J. Feng, Q. Huo, N. Melosh, G. H. Fredrickson, B. F. Chmelka and G. D. Stucky, *Science*, 1998, **279**, 548–552; (*d*) D. Zhao, Q. Huo, J. Feng, B. F. Chmelka and G. D. Stucky, *J. Am. Chem. Soc.*, 1998, **120**, 6024–6036; (*e*) J. Fan, C. Yu, J. Lei, Q. Zhang, T. Li, B. Tu, W. Zhou and D. Zhao, *J. Am. Chem. Soc.*, 2005, **127**, 10794–10795.
2 G. J. A. A. Soler-Illia, C. Sanchez, B. Lebeau and J. Patarin, *Chem. Rev.*, 2002, **102**, 4093–4138.
3 (*a*) P. K. Thallapally, B. P. Mcgrail, S. J. Dalgarno, H. T. Schaef, J. Tian and J. L. Atwood, *Nat. Mater.*, 2008, **7**, 146–150; (*b*) B. D. Chandler, G. D. Enright, K. A. Udachin, S. Pawsey, J. A. Ripmeester, D. T. Cramb and G. K. H. Shimizu, *Nat. Mater.*, 2008, **7**, 229–235.
4 J. Lee, M. C. Orilall, S. C. Warren, M. Kamperman, F. J. Disalvo and U. Wiesner, *Nat. Mater.*, 2008, **7**, 222–228.
5 Z. Y. Yuan and B. L. Su, *J. Mater. Chem.*, 2006, **16**, 663–677.
6 E. Galli and A. F. Gualtieri, *Am. Mineral.*, 2008, **93**, 95–102.
7 P. M. Budd, *Science*, 2007, **316**, 210–211.
8 T. Uemura, Y. Kadowaki, N. Yanai and S. Kitagawa, *Chem. Mater.*, 2009, **21**, 4096–4098.
9 (*a*) C. T. Kresge, M. E. Leonowicz, W. J. Roth, J. C. Vartuli and J. S. Beck, *Nature*, 1992, **359**, 710–712; (*b*) J. S. Beck, J. C. Vartuli, W. J. Roth, M. E. Leonowicz, C. T. Kresge, K. D. Schmitt, C. T.-W. Chu, D. H. Olsen, E. W. Sheppard, S. B. McCullen, J. B. Higgins and J. L. Schlenker, *J. Am. Chem. Soc.*, 1992, **114**, 10834–10843.
10 (*a*) B. T. Holland, C. F. Blanford and A. Stein, *Science*, 1998, **281**, 538–540; (*b*) C. F. Blanford, H. Yan, R. C. Schroden, M. Al-Daous and A. Stein, *Adv. Mater.*, 2001, **13**, 401–407; (*c*) H. W. Yan,

C. F. Blanford, B. T. Holland, W. H. Smyrl and A. Stein, *Chem. Mater.*, 2000, **12**, 1134–1141.
11 H. M. El-Kaderi, J. R. Hunt, J. L. Mendoza-Cortés, A. P. Côté, R. E. Taylor, M. O'Keeffe and O. M. Yaghi, *Science*, 2007, **316**, 268–272.
12 (*a*) D. Haldar, A. Banerjee, M. G. B. Drew, A. K. Das and A. Banerjee, *Chem.Commun.*, 2003, 1406–1407; (*b*) S. Ray, D. Haldar, M. G. B. Drew and A. Banerjee, *Org. Lett.*, 2004, **6**, 4463–4465; (*c*) D. Haldar, H. Jiang, J.-M. Léger and I. Huc, *Tetrahedron*, 2007, **63**, 6322–6330; (*d*) D. Haldar, H. Jiang, J.-M. Léger and I. Huc, *Angew. Chem., Int. Ed.*, 2006, **45**, 5483–5486.
13 (*a*) A. P. Alivastos, K. P. Johnson, X. Peng, T. E. Wilson, C. J. Loweth, M. P. Bruchez and P. G. Schultz, *Nature*, 1996, **382**, 609–611; (*b*) S. Mann, W. Shenton, M. Li, S. Connolly and D. Fitzmaurice, *Adv. Mater.*, 2000, **12**, 147–150.
14 J. R. Krenn, B. Lamprecht, H. Ditlbacher, G. Schider, M. Salerno, A. Leitner and F. R. Aussenegg, *Europhys. Lett.*, 2002, **60**, 663–669.
15 J. J. Storhoff, R. Elghanian, R. C. Mucic, C. A. Mirkin and R. L. Letsinger, *J. Am. Chem. Soc.*, 1998, **120**, 1959–1964.
16 A. Gole, C. Dash, V. Ramakrishnan, S. R. Sainkar, A. B. Mandale, M. Rao and M. Sastry, *Langmuir*, 2001, **17**, 1674–1679.
17 (*a*) J. Puigmartí-Luis, Á. P. del Pino, E. Laukhina, J. Esquena, V. Laukhin, C. Rovira, J. Vidal-Gancedo, A. G. Kanaras, R. J. Nichols, M. Brust and D. B. Amabilino, *Angew. Chem., Int. Ed.*, 2008, **47**, 1861–1865; (*b*) A. Pal, A. Srivastava and S. Bhattacharya, *Chem.–Eur. J.*, 2009, **15**, 9169–9182.
18 C. A. Mirkin, R. L. Letsinger, R. C. Mucic and J. J. Storhoff, *Nature*, 1996, **382**, 607–609.
19 (*a*) Y. Zhou, W. Chen, H. Itoh, K. Naka, Q. Ni, H. Yamane and Y. Chujo, *Chem. Commun.*, 2001, 2518–2519; (*b*) R. R. Bhattacharjee, A. K. Das, D. Haldar, S. Si, A. Banerjee and T. K. Mandal, *J. Nanosci. Nanotechnol.*, 2005, **5**, 1141–1147.
20 M. Bodanszky, A. Bodanszky, *The Practice of Peptide Synthesis,*Springer-Verlag, New York, 1984; pp. 1–282.
21 D. Haldar, M. G. B. Drew and A. Banerjee, *Tetrahedron*, 2006, **62**, 6370–6378.
22 (*a*) C. Toniolo and M. Palumbo, *Biopolymers*, 1977, **16**, 219–224; (*b*) V. Moretto, M. Crisma, G. M. Bonora, C. Toniolo, H. Balaram and P. Balaram, *Macromolecules*, 1989, **22**, 2939–2944; (*c*) D. Haldar and A. Banerjee, *Int. J. Pept. Res. Ther.*, 2007, **13**, 439–446.
23 (*a*) G. P. Dado and S. H. Gellman, *J. Am. Chem. Soc.*, 1994, **116**, 1054–1062; (*b*) D. Haldar and A. Banerjee, *Int. J. Pept. Res. Ther.*, 2006, **12**, 341–348.
24 (*a*) S. E. Blondelle, B. Forood, A. R. Houghten and E. Peraz-Paya, *Biochemistry*, 1997, **36**, 8393–8400; (*b*) P. I. Haris and D. Chapman, *Biopolymers*, 1995, **37**, 251–263.
25 D. Haldar, M. G. B. Drew and A. Banerjee, *Tetrahedron*, 2007, **63**, 5561–5566.
26 B. Adhikari, G. Palui and A. Banerjee, *Soft Matter*, 2009, **5**, 3452–3460.
27 D. Chandra, B. K. Jena, C. R. Raj and A. Bhaumik, *Chem. Mater.*, 2007, **19**, 6290–6296.
28 D. Chandra and A. Bhaumik, *J. Mater. Chem.*, 2009, **19**, 1901–1907.
29 S. Si, R. R. Bhattacharjee, A. Banerjee and T. K. Mandal, *Chem.–Eur. J.*, 2006, **12**, 1256–1265.
30 G. M. Sheldrick, *SHELX 97*, University of Göttingen, Germany, 1997.

